第 35 卷第 3 期 无 机 化 学 学 报 Vol.35 No.3
2019 年 3 月 CHINESE JOURNAL OF INORGANIC CHEMISTRY 505-514

基于 5-氯烟酸的镍(Ⅱ)和锌(Ⅱ)配位聚合物的合成、晶体结构、荧光和磁性质

陈金伟[1] 黎 彧*,[2] 邹训重[2] 邱文达[2] 成晓玲*,[3]
([1]广东轻工职业技术学院轻化工技术学院,广州 510300)
([2]广东轻工职业技术学院广东省特种建筑材料及其绿色制备工程技术研究中心/佛山市特种功能性建筑材料及其绿色制备技术工程中心,广州 510300)
([3]广东工业大学轻工化工学院,广州 510006)

摘要:利用水热方法,以 5-氯烟酸(5-ClnicH)和菲咯啉(phen)或 2,2′-联咪唑(H_2biim)分别与 $NiCl_2\cdot 6H_2O$ 和 $ZnCl_2$ 反应,合成了 1 个三维配位聚合物{[Ni(μ-5-Clnic)(μ_3-5-Clnic)(μ-H_2O)$_{0.5}$]$\cdot$1.5H_2O}$_n$ (**1**)以及 3 个一维链状配位聚合物[Ni(5-Clnic)(μ-5-Clnic)(H_2biim)]$_n$ (**2**)、[Zn(5-Clnic)(μ-5-Clnic)(H_2biim)]$_n$ (**3**)和{[Zn(5-Clnic)(μ-5-Clnic)(phen)]$\cdot$2H_2O}$_n$ (**4**),并对其结构、荧光和磁性质进行了研究。结构分析结果表明 4 个配位聚合物分别属于单斜、正交(**2**、**3**)和三斜晶系,*I*2/*a*、*Pbcn*(**2**、**3**)和 $P\bar{1}$ 空间群。配合物 **1** 具有基于双核单元的三维框架结构,而配合物 **2~4** 呈现一维链结构。这些一维链通过链间 N–H…O 氢键和 Cl…Cl 卤键作用进一步连接成了二维网络和三维超分子框架结构。研究表明,聚合物 **1** 和 **2** 中相邻 Ni(Ⅱ)离子间存在反铁磁相互作用,配合物 **3** 和 **4** 在室温下能发出蓝色荧光。

关键词:配位聚合物;卤键;5-氯烟酸;磁性;荧光
中图分类号:O614.81$^+$3;O614.24$^+$1 **文献标识码**:A **文章编号**:1001-4861(2019)03-0505-10
DOI:10.11862/CJIC.2019.048

Syntheses, Crystal Structures, Luminescent and Magnetic Properties of Nickel(Ⅱ) and Zinc(Ⅱ) Coordination Polymers Constructed from 5-Chloronicotinic Acid

CHEN Jin-Wei[1] LI Yu*,[2] ZOU Xun-Zhong[2] QIU Wen-Da[2] CHENG Xiao-Ling*,[3]
([1]*School of Light Chemical Engineering, Guangdong Industry Polytechnic, Guangzhou* 510300, *China*)
([2]*Guangdong Research Center for Special Building Materials and Its Green Preparation Technology/Foshan Research Center for Special Functional Building Materials and Its Green Preparation Technology, Guangdong Industry Polytechnic, Guangzhou* 510300, *China*)
([3]*School of Chemical Engineering and Light Industry, Guangdong University of Techlonogy, Guangzhou* 510006, *China*)

Abstract: Two nickel(Ⅱ) and two zinc(Ⅱ) coordination polymers, namely {[Ni(μ-5-Clnic)(μ_3-5-Clnic)(μ-H_2O)$_{0.5}$]$\cdot$1.5H_2O}$_n$ (**1**), [Ni(5-Clnic)(μ-5-Clnic)(H_2biim)]$_n$ (**2**), [Zn(5-Clnic)(μ-5-Clnic)(H_2biim)]$_n$ (**3**) and {[Zn(5-Clnic)(μ-5-Clnic)(phen)]$\cdot$2H_2O}$_n$ (**4**), have been constructed hydrothermally using 5-ClnicH (5-ClnicH=5-chloronicotinic acid), phen (phen=1,10-phenanthroline), H_2biim (H_2biim=2,2′-biimidazole), and nickel or zinc chlorides. Single-crystal X-ray diffraction analyses revealed that four polymers crystallize in the monoclinic, orthorhombic (**2**, **3**) or triclinic systems, space groups *I*2/*a*, *Pbcn* (**2**, **3**) or $P\bar{1}$. Polymer **1** possesses a 3D metal-organic framework based on dinuclear units. Polymers **2~4** show 1D chains, which are further extended into a 2D supramolecular network or

收稿日期:2018-08-21。收修改稿日期:2018-10-20。
广东省高等职业院校珠江学者岗位计划资助项目(2015,2018),广东省自然科学基金(No.2016A030313761),广东轻院珠江学者人才类项目(No.RC2015-001),生物无机与合成化学教育部重点实验室开放基金(2016),广东省高校创新团队项目(No.2017GKCXTD001),广州市科技计划项目(2019),广东省高校特色创新项目(No.2017GKTSCX005),广东轻院拔尖人才项目(No.IB040103)和广东轻院科技成果培育项目(No.KJPY002)资助。
*通信联系人。E-mail:liyuletter@163.com,ggcxl@163.com

3D supramolecular framework through N–H···O hydrogen bonds or Cl···Cl interactions. Magnetic and luminescent properties of all compounds have been studied. CCDC: 1859598, **1**; 1859599, **2**; 1859600, **3**; 1859601, **4**.

Keywords: coordination polymer; halogen bonding; 5-chloronicotinic acid; magnetic properties; luminescent properties

0 Introduction

The design and hydrothermal syntheses of metal-organic coordination polymers have attracted great interest in the field of coordination chemistry and organic chemistry owing to their intriguing architectures and topologies, as well as potential applications in catalysis, magnetism, luminescence and gas absorption[1-6]. There are many factors, such as the coordination geometry of the metal centers, type and connectivity of organic ligands, stoichiometry, reaction conditions, template effect, presence of auxiliary ligands, and pH values influencing the structures of target coordination polymers during self-assembly[7-12]. Among these factors, organic ligands play a very important role in constructing coordination polymers.

As we known, the carboxylate ligands have been certified to be of great significance as constructors due to their abundant coordination modes, which could satisfy different geometric requirements of metal centers[13-18]. Apart from carboxylate ligands, 1,10-phenanthroline (phen) and 2,2′-biimidazole (H_2biim) have often been used as secondary N,N-donor building blocks to construct and stabilize new structures, on account of their effective $\pi\cdots\pi$ stacking and/or weak H-bonding interactions[15-18]. As a continuation of our research in this field, we have tested the hydrothermal self-assembly reactions of nickel and zinc chlorides with 5-chloronicotinic acid (5-Clnic) as a main building block and 1,10-phenanthroline or 2,2′-biimidazole as *N*,*N*-donor anxiliary ligands in view of the following considerations: (A) an availability of pyridyl N and carboxylate O atoms for the coordination to a metal center, (B) the presence of Cl-functionality that is capable of taking part in Cl ··· Cl interaction, (C) facilitating the crystallization of compounds and stabilization of their structures by the introduction of phen and H_2biim ligands.

Taking into consideration the above discussion, we herein report the syntheses, crystal structures, magnetic and luminescent properties of four Ni(Ⅱ) and Zinc(Ⅱ) coordination polymers constructed from 5-chloronicotinic acid ligand.

1 Experimental

1.1 Reagents and physical measurement

All chemicals and solvents were of AR grade and used without further purification. Carbon, hydrogen and nitrogen were determined using an Elementar Vario EL elemental analyzer. IR spectra were recorded using KBr pellets and a Bruker EQUINOX 55 spectrometer. Thermogravimetric analysis (TGA) data were collected on a LINSEIS STA PT1600 thermal analyzer with a heating rate of 10 ℃·min^{-1}. Magnetic susceptibility data were collected in a temperature range of 2 ~300 K with a Quantum Design SQUID Magnetometer MPMS XL-7 with a field of 0.1 T. A correction was made for the diamagnetic contribution prior to data analysis. Excitation and emission spectra were recorded for the solid samples on an Edinburgh FLS920 fluorescence spectrometer at room temperature.

1.2 Synthesis of {[Ni(μ-5-Clnic)(μ_3-5-Clnic)(μ-H_2O)$_{0.5}$]·1.5H_2O}$_n$ (1)

A mixture of $NiCl_2\cdot 6H_2O$ (0.025 g, 0.10 mmol), 5-ClnicH (0.032 g, 0.20 mmol), NaOH (0.008 g, 0.20 mmol), and H_2O (10 mL) was stirred at room temperature for 15 min, and then sealed in a 25 mL Teflon-lined stainless steel vessel, and heated at 160 ℃ for 3 days, followed by cooling to room temperature at a rate of 10 ℃·h^{-1}. Green block-shaped crystals of **1** were isolated manually, and washed with distilled water. Yield: 71% (based on 5-ClnicH). Anal. Calcd. for $C_{12}H_{10}Cl_2NiN_2O_6$(%): C 35.34, H 2.47, N 6.87; Found (%): C 35.22, H 2.46, N 6.91. IR (KBr, cm^{-1}): 3 434w, 3 125w, 1 632m, 1 562 w, 1 528w, 1 457w, 1 394s, 1 289w, 1 236w, 1 131w, 1 097w, 1 026w,

909w, 782w, 746m, 688w, 589w.

1.3 Synthesis of [Ni(5-Clnic)(μ-5-Clnic)(H$_2$biim)]$_n$ (2)

The synthesis of complex **2** is same to **1** except that H$_2$biim (0.014 g, 0.1 mmol) is added. Blue block-shaped crystals of **2** were isolated manually, and washed with distilled water. Yield: 62% (based on 5-ClnicH). Anal. Calcd. for $C_{18}H_{12}Cl_2NiN_6O_4$(%): C 42.73, H 2.39, N 16.61; Found(%): C 42.61, H 2.41, N 16.85. IR (KBr, cm^{-1}): 1 609s, 1 551w, 1 452w, 1 388s, 1 370m, 1 335w, 1 277w, 1 189w, 1 125m, 1 026w, 991w, 927w, 898w, 782m, 752w, 688w, 595w.

1.4 Synthesis of [Zn(5-Clnic)(μ-5-Clnic)(H$_2$biim)]$_n$ (3)

Synthesis of **3** was similar to **2** except using $ZnCl_2$ (0.014 g, 0.10 mmol) instead of $NiCl_2\cdot 6H_2O$. Colorless block-shaped crystals of **3** were isolated manually, and washed with distilled water. Yield 55% (based on Zn). Colorless block-shaped crystals of **3** were isolated manually, and washed with distilled water. Yield: 65% (based on 5-ClnicH). Anal. Calcd. for $C_{18}H_{12}Cl_2ZnN_6O_4$ (%): C 42.17, H 2.36, N 16.39; Found(%): C 42.34, H 2.37, N 16.53. IR (KBr, cm^{-1}): 1 609s, 1 556w, 1 440w, 1 394s, 1 370s, 1 329w, 1 283w, 1 189w, 1 125m, 1 032 w, 991w, 898w, 782m, 752w, 729w, 688w.

1.5 Synthesis of {[Zn(5-Clnic)(μ-5-Clnic)(phen)]·2H$_2$O}$_n$ (4)

Synthesis of **4** was similar to **3** except using phen (0.020 g, 0.10 mmol) instead of H$_2$biim. Colorless block-shaped crystals of **4** were isolated manually, and washed with distilled water. Yield: 60% (based on 5-ClnicH). Anal. Calcd. for $C_{24}H_{18}Cl_2ZnN_4O_6$(%): C 48.47, H 3.05, N 9.42; Found(%): C 48.35, H 3.07, N 9.50. IR (KBr, cm^{-1}): 3 438w, 3 097w, 1 628s, 1 561m, 1 510w, 1 423w, 1 393s, 1 291w, 1 225w, 1 184w, 1 133w, 1 102 w, 1 026w, 898w, 847w, 786w, 750w, 724m, 684w, 638w. The compounds are insoluble in water and common organic solvents, such as methanol, ethanol, acetone, and DMF.

1.6 Structure determination

Four single crystals with dimensions of 0.26 mm×0.21 mm×0.20 mm (**1**), 0.28 mm×0.26 mm×0.25 mm (**2**), 0.27 mm×0.23 mm×0.22 mm (**3**), and 0.25 mm×0.23 mm×0.21 mm (**4**) were collected at 293(2) K on a Bruker SMART APEX Ⅱ CCD diffractometer with Mo $K\alpha$ radiation (λ=0.071 073 nm). The structures were solved by direct methods and refined by full matrix least-square on F^2 using the SHELXTL-2014 program[19]. All non-hydrogen atoms were refined anisotropically. All the hydrogen atoms were positioned geometrically and refined using a riding model. Some lattice solvent molecules in **1** are highly disordered and were removed using the SQUEEZE routine in PLATON[20]. The number of solvent H$_2$O molecules was obtained on the basis of elemental and thermogravimetric analyses. A summary of the crystallography data and structure refinements for **1**~**4** is given in Table 1. The selected bond lengths and angles for compounds **1**~**4** are listed in Table 2. Hydrogen bond parameters of compounds **1**~**4** are given in Table 3.

CCDC: 1859598, **1**; 1859599, **2**; 1859600, **3**; 1859601, **4**.

Table 1　Crystal data for compounds 1~4

Compound	1	2	3	4
Chemical formula	$C_{12}H_{10}Cl_2NiN_2O_6$	$C_{18}H_{12}Cl_2NiN_6O_4$	$C_{18}H_{12}Cl_2ZnN_6O_4$	$C_{24}H_{18}Cl_2ZnN_4O_6$
Molecular weight	407.81	505.95	512.61	594.69
Crystal system	Monoclinic	Orthorhombic	Orthorhombic	Triclinic
Space group	*I*2/*a*	*Pbcn*	*Pbcn*	$P\bar{1}$
a / nm	1.432 71(16)	0.778 75(3)	0.779 11(3)	0.771 48(8)
b / nm	1.672 20(16)	1.804 37(7)	1.827 48(8)	1.264 3(2)
c / nm	1.462 59(17)	2.758 83(11)	2.777 68(13)	1.328 8(2)
α / (°)				106.443(16)
β / (°)	118.373(14)			90.973(11)
γ / (°)				90.282(12)

Continued Table 1

V / nm^3	3.083 1(7)	3.876 6(3)	3.954 9(3)	1.242 8(4)
Z	8	8	8	2
F(000)	1 528	2 048	2 064	604
θ range for data collection / (°)	3.673~25.049	3.534~25.047	3.514~25.046	3.280~25.049
Limiting indices	$-16 \leqslant h \leqslant 17$, $-19 \leqslant k \leqslant 16$, $-17 \leqslant l \leqslant 14$	$-9 \leqslant h \leqslant 9$, $-20 \leqslant k \leqslant 21$, $-32 \leqslant l \leqslant 18$	$-9 \leqslant h \leqslant 8$, $-21 \leqslant k \leqslant 19$, $-31 \leqslant l \leqslant 33$	$-8 \leqslant h \leqslant 9$, $-15 \leqslant k \leqslant 9$, $-13 \leqslant l \leqslant 15$
Reflection collected, unique (R_{int})	5 459, 2 730 (0.052 0)	13 122, 3 432 (0.059 8)	13 633, 3 495 (0.063 9)	7 527, 4 396 (0.070 9)
D_c / (g·cm^{-3})	1.641	1.734	1.722	1.589
μ / mm^{-1}	1.623	1.318	1.553	1.251
Data, restraint, parameter	2 730, 0, 195	3 432, 0, 280	3 495, 0, 284	4 396, 0, 334
Goodness-of-fit on F^2	1.029	1.032	1.052	1.012
Final R indices [$I \geqslant 2\sigma(I)$] R_1, wR_2	0.052 8, 0.100 0	0.040 5, 0.085 6	0.044 3, 0.086 0	0.073 2, 0.141 0
R indices (all data) R_1, wR_2	0.079 2, 0.112 4	0.065 0, 0.102 2	0.069 6, 0.101 7	0.133 7, 0.183 6
Largest diff. peak and hole / (e·nm^{-3})	811 and −566	411 and −436	478 and −437	490 and −712

Table 2 Selected bond distances (nm) and bond angles (°) for compounds 1~4

		1			
Ni(1)-O(1)A	0.212 5(3)	Ni(1)-O(3)	0.206 0(3)	Ni(1)-O(4)B	0.205 8(3)
Ni(1)-O(5)	0.208 6(2)	Ni(1)-N(1)	0.210 4(4)	Ni(1)-N(2)C	0.208 1(4)
O(4)B-Ni(1)-O(3)	96.65(13)	O(4)B-Ni(1)-N(2)C	91.38(14)	O(3)-Ni(1)-N(2)C	84.76(14)
O(4)B-Ni(1)-O(5)	87.91(10)	O(3)-Ni(1)-O(5)	91.24(12)	O(5)-Ni(1)-N(2)C	175.83(15)
O(4)B-Ni(1)-N(1)	88.96(14)	O(3)-Ni(1)-N(1)	170.91(13)	N(1)-Ni(1)-N(2)C	87.98(15)
O(5)-Ni(1)-N(1)	96.12(14)	O(4)B-Ni(1)-O(1)A	177.41(12)	O(3)-Ni(1)-O(1)A	83.90(13)
N(2)C-Ni(1)-O(1)A	91.19(14)	O(5)-Ni(1)-O(1)A	89.54(10)	N(1)-Ni(1)-O(1)A	90.82(14)
Ni(1)-O(5)-Ni(1)B	113.9(2)				
		2			
Ni(1)-O(3)A	0.218 1(2)	Ni(1)-O(4)A	0.212 0(2)	Ni(1)-N(1)	0.209 7(3)
Ni(1)-N(2)	0.210 7(3)	Ni(1)-N(3)	0.208 5(3)	Ni(1)-N(6)	0.205 1(3)
N(6)-Ni(1)-N(3)	80.37(12)	N(6)-Ni(1)-N(1)	90.67(12)	N(3)-Ni(1)-N(1)	170.17(12)
N(6)-Ni(1)-N(2)	97.36(11)	N(3)-Ni(1)-N(2)	89.95(12)	N(2)-Ni(1)-N(1)	95.24(11)
N(6)-Ni(1)-O(4)A	168.24(11)	N(3)-Ni(1)-O(4)A	95.20(11)	N(1)-Ni(1)-O(4)A	92.82(11)
N(2)-Ni(1)-O(4)A	93.50(10)	N(6)-Ni(1)-O(3)A	107.57(11)	N(3)-Ni(1)-O(3)A	92.45(11)
N(1)-Ni(1)-O(3)A	86.37(10)	N(2)-Ni(1)-O(3)A	155.01(11)	O(3)A-Ni(1)-O(4)A	61.51(9)
		3			
Zn(1)-O(3)A	0.218 2(3)	Zn(1)-O(4)A	0.225 6(3)	Zn(1)-N(1)	0.216 6(3)
Zn(1)-N(2)	0.216 9(3)	Zn(1)-N(3)	0.208 0(3)	Zn(1)-N(6)	0.213 6(3)
N(3)-Zn(1)-N(6)	79.81(13)	N(3)-Zn(1)-N(1)	90.70(13)	N(6)-Zn(1)-N(1)	170.13(14)
N(3)-Zn(1)-N(2)	101.00(12)	N(6)-Zn(1)-N(2)	90.43(13)	N(1)-Zn(1)-N(2)	94.07(12)
N(3)-Zn(1)-O(3)A	110.92(12)	N(6)-Zn(1)-O(3)A	94.21(11)	N(1)-Zn(1)-O(3)A	86.60(11)
N(2)-Zn(1)-O(3)A	148.06(12)	N(3)-Zn(1)-O(4)A	169.12(12)	N(6)-Zn(1)-O(4)A	95.64(12)
N(1)-Zn(1)-O(4)A	93.23(12)	N(2)-Zn(1)-O(4)A	88.85(11)	O(3)A-Zn(1)-O(4)A	59.27(10)

Continued Table 2

4					
Zn(1)-O(1)	0.212 8(5)	Zn(1)-O(2)	0.238 4(6)	Zn(1)-O(3)	0.205 4(5)
Zn(1)-N(1)A	0.212 5(5)	Zn(1)-N(3)	0.223 8(6)	Zn(1)-N(4)	0.212 7(6)
O(3)-Zn(1)-N(1)A	92.6(2)	O(3)-Zn(1)-N(4)	89.3(2)	N(1)A-Zn(1)-N(4)	108.1(2)
O(3)-Zn(1)-O(1)	94.72(19)	N(1)A-Zn(1)-O(1)	144.4(2)	N(4)-Zn(1)-O(1)	106.8(2)
O(3)-Zn(1)-N(3)	165.3(2)	N(1)-Zn(1)-N(3)	88.2(2)	N(4)-Zn(1)-N(3)	76.5(2)
O(1)-Zn(1)-N(3)	93.21(19)	O(3)-Zn(1)-O(2)	112.1(2)	N(1)-Zn(1)-O(2)	86.7(2)
N(4)-Zn(1)-O(2)	153.7(2)	O(2)-Zn(1)-O(1)	58.30(19)	N(3)-Zn(1)-O(2)	82.6(2)

Symmetry codes: A: x, $-y+1/2$, $z-1/2$; B: $-x+1/2$, y, $-z$; C: $-x+1$, $-y+1$, $-z$ for **1**; A: $x+1$, y, z for **2**; A: $x+1$, y, z for **3**; A: $x-1$, y, z for **4**.

Table 3　Hydrogen bond lengths (nm) and angles (°) of compounds 1 and 2

Compound	D–H···A	d(D-H) / nm	d(H···A) / nm	d(D···A) / nm	∠DHA / (°)
1	O(5)–H(1W)···O(2)A	0.085	0.166	0.251 4	179.7
	O(5)–H(2W)···O(2)B	0.085	0.166	0.251 4	179.7
2	N(4)–H(1)···O(2)A	0.086	0.185	0.270 9	172.6
	N(5)–H(2)···O(1)A	0.086	0.180	0.265 4	175.2
3	N(4)–H(1)···O(1)A	0.086	0.178	0.263 6	174.1
	N(5)–H(2)···O(2)A	0.085	0.185	0.270 0	170.9
4	O(5)–H(1W)···O(4)A	0.085	0.196	0.281 1	179.3
	O(5)–H(2W)···N(2)B	0.085	0.202	0.286 9	173.1
	O(6)–H(3W)···O(5)C	0.085	0.208	0.293 1	179.0

Symmetry codes: A: $-x+1/2$, $-y+1/2$, $-z+1/2$; B: x, $-y+1/2$, $-z+1/2$ for **1**; A: $x-1/2$, $y+1/2$, $-z+3/2$ for **2**.

2　Results and discussion

2.1　Description of the structure

2.1.1　$\{[Ni(\mu\text{-}5\text{-}Clnic)(\mu_3\text{-}5\text{-}Clnic)(\mu\text{-}H_2O)_{0.5}]\cdot 1.5H_2O\}_n$ (**1**)

Compound **1** has a 3D metal-organic framework structure. The asymmetric unit of **1** (Fig.1) comprises one Ni(Ⅱ) ion, two μ-5-Clnic$^-$ and μ_3-5-Clnic$^-$ ligands, and a half of H_2O ligand that is positioned on a 2-fold rotation axis. The six-coordinated Ni1 ion is surrounded by three O atoms of three different 5-Clnic$^-$ blocks, one O atom of H_2O ligand, and two N atoms of two individual 5-Clnic$^-$ moieties, constructing a slightly distorted $\{NiN_2O_4\}$ octahedral geometry. The Ni-O (0.205 8(3)~0.212 5(3) nm) and Ni-N (0.208 1(4)~0.210 4(4) nm) bond lengths are in good agreement with those observed in some other Ni(Ⅱ) compounds[17-18,21]. In **1**, the 5-Clnic$^-$ blocks take μ- and μ_3-coordination modes (modes Ⅰ and Ⅱ, Scheme 1), in which the carboxylate groups act in η^1:η^0 monodentate and μ_2-η^1:η^1 bidentate modes, respectively. Two Ni1 centers are bridged by two carboxylate groups and one μ-H_2O ligand, giving rise to a binuclear Ni_2 unit (Fig.2) with a Ni···Ni separation of 0.349 7(4) nm and a Ni-O_{water}-Ni angle of 113.9(2)°. The adjacent Ni_2 units are multiply interlinked by the 5-Clnic$^-$ blocks to form an intricate 3D framework (Fig.3). Interestingly, in the MOF **1** the distance between the adjacent Cl atoms is 0.342 4(4) nm, which is shorter than the sum of the van der Waals radii of the two Cl atoms (*ca.* 0.350 nm)[22],

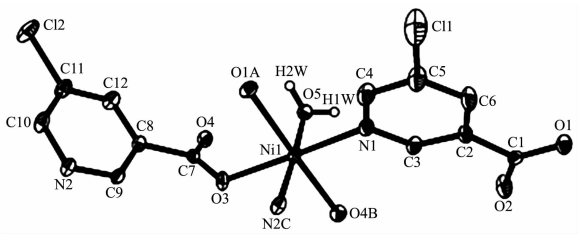

H atoms and lattice water molecules were omitted for clarity except H of H_2O ligand; Symmetry codes: A: x, $-y+1/2$, $z-1/2$; B: $-x+1/2$, y, $-z$; C: $-x+1$, $-y+1$, $-z$

Fig.1　Drawing of asymmetric unit of compound **1** with 30% probability thermal ellipsoids

thus indicating the existence of the Cl ⋯ Cl interactions (Fig.3).

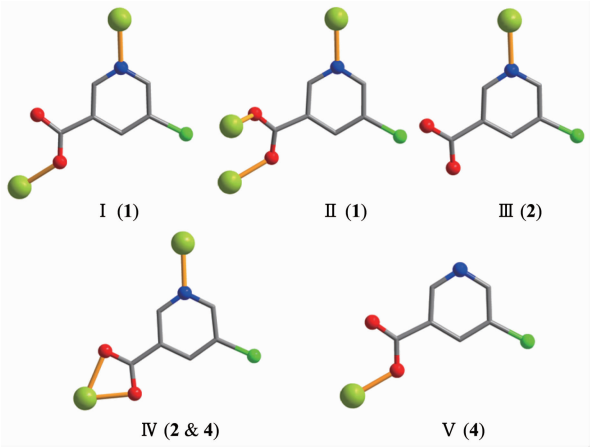

Scheme 1 Coordination modes of Clnic⁻ ligands in compounds **1**~**4**

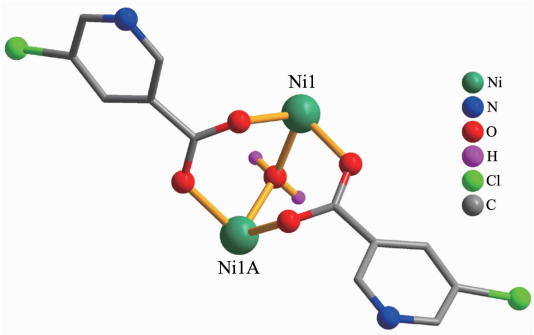

Symmetry codes: A: $-x+1/2, y, -z$

Fig.2 Di-nickel(Ⅱ) unit of **1**

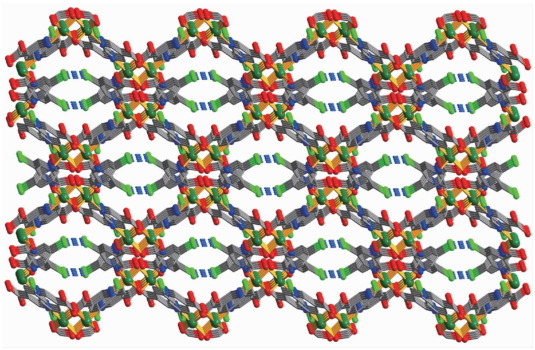

Dashed lines: Cl⋯Cl interactions

Fig.3 Perspective of a 3D framework of **1** parallel to *bc* plane

2.1.2 [Ni(5-Clnic)(μ-5-Clnic)(H_2biim)]$_n$ (**2**) and [Zn(5-Clnic)(μ-5-Clnic)(H_2biim)]$_n$ (**3**)

Compounds **2** and **3** are isostructural and feature a 1D metal-organic chain. As a representative example, the structure of **2** is described in detail (Fig.4). The asymmetric unit of compound **2** contains one crystallographically unique Ni(Ⅱ) ion, two distinct 5-Clnic⁻ and μ-5-Clnic⁻ ligands, and one H_2biim moiety. As depicted in Fig.4, each Ni(Ⅱ) ion is six-coordinated and adopts a distorted octahedral {NiN_4O_2} geometry formed by two carboxylate O atoms of one μ-5-Clnic⁻ block, two N atoms of two different 5-Clnic⁻ and μ-5-Clnic⁻ ligands as well as two N atoms of one H_2biim moiety. The Ni-O (0.212 0(2)~0.218 1(2) nm) and Ni-N (0.205 1(3)~0.210 7(3) nm) bond lengths are comparable to the literature data[15,17,21]. In **2**, the 5-Clnic⁻ ligands exhibit two different terminal and μ-coordination modes (modes Ⅲ and Ⅳ, Scheme 1), in which the carboxylate group either shows a η^1:η^1 bidentate mode or remains uncoordinated. The H_2biim ligand acts in a bidentate chelating mode; the dihedral angle of two imidazole groups is 1.17°. The μ-5-Clnic⁻ moieties alternatively link the adjacent Ni(Ⅱ) centers to form a linear 1D metal-organic chain with the Ni ⋯ Ni separation of 0.778 7(3) nm (Fig.5). The neighboring chains are assembled into 2D supramolecular sheet motifs through the N–H⋯O hydrogen bonds (Fig.6).

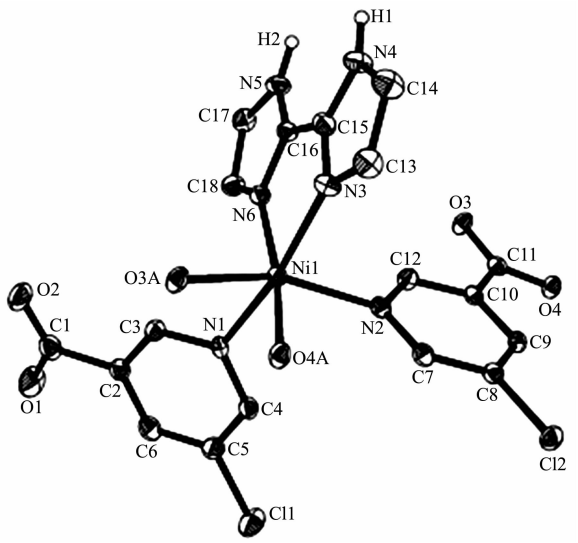

H atoms were omitted for clarity except those bonded to N atoms; Symmetry codes: A: $x+1, y, z$

Fig.4 Drawing of asymmetric unit of compound **2** with 30% probability thermal ellipsoids

2.1.3 {[Zn(5-Clnic)(μ-5-Clnic)(phen)]·2H_2O}$_n$ (**4**)

The compound **4** crystallizes in the triclinic space group $P\bar{1}$ and also shows a linear 1D metal-

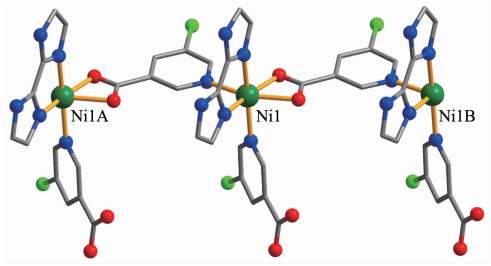

Symmetry codes: A: $x-1$, y, z; B: $x+1$, y, z

Fig.5　Perspective view of 1D chain along c axis

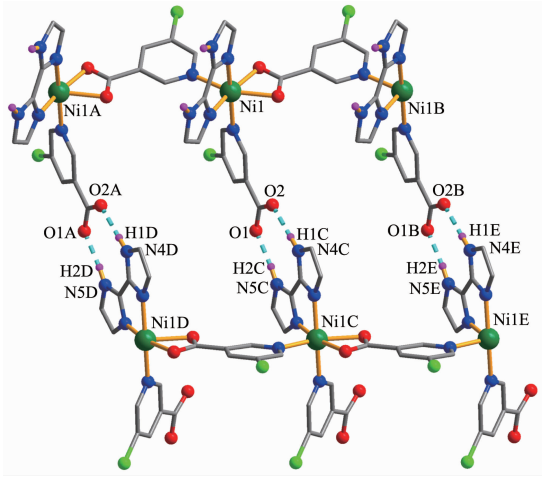

Dashed lines: H-bonds; Symmetry codes: A: $x-1$, y, z; B: $x+1$, y, z; C: $x+1/2$, $y-1/2$, $-z+3/2$; D: $x-1/2$, $y-1/2$, $-z+3/2$; E: $x+3/2$, $y-1/2$, $-z+3/2$

Fig.6　Perspective of a 2D supramolecular network along a axis

organic chain structure. The asymmetric unit bears one crystallographically independent Zn(Ⅱ) ion, one terminal 5-Clnic$^-$ and one μ-5-Clnic$^-$ block, one phen ligand, and two lattice water molecules. As depicted in Fig.7, the six-coordinated Zn(Ⅱ) ion adopts a distorted octahedral $\{ZnN_3O_3\}$ geometry taken by three O atoms from the two distinct 5-Clnic$^-$ moieties and three N atoms from one 5-Clnic$^-$ and one phen ligand. The Zn-O and Zn-N bond distances are in ranges of 0.205 4(5)~0.238 4(6) nm and 0.212 5(5)~0.223 8(6) nm, which are within typical values for the Zn(Ⅱ)derivatives[16,23-24]. In **4**, the 5-Clnic$^-$ ligands show two different coordination modes (modes Ⅳ and Ⅴ, Scheme 1), in which the carboxylate groups are either η^1:η^0 monodentate or η^1:η^1 bidentate. It should be mentioned that the N atom of 5-Clnic$^-$ remains uncoordinated in the mode Ⅴ. The μ-5-Clnic$^-$ moieties alternately bridge the adjacent Zn(Ⅱ) centers to form a linear 1D metal-organic chain (Fig.8). The neighboring chains are sewed up into 3D supramolecular framework through Cl⋯Cl (0.331 6(5) nm) interactions and O–H⋯O hydrogen bonds involving lattice water molecules (Fig.9).

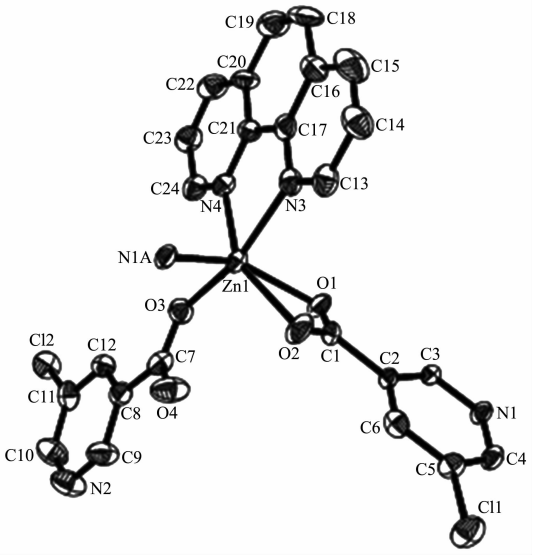

H atoms were omitted for clarity; Symmetry codes: A: $x-1$, y, z

Fig.7　Drawing of asymmetric unit of compound **4** with 30% probability thermal ellipsoids

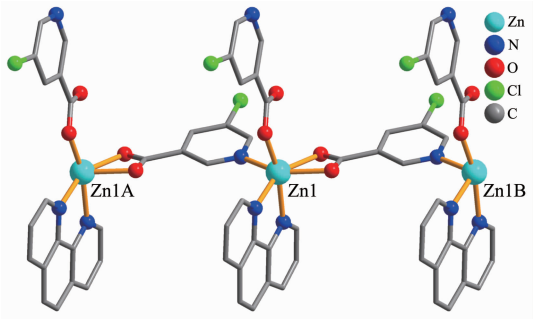

Symmetry codes: A: $x-1$, y, z; B: $x+1$, y, z

Fig.8　One dimensional chain in compound **4**

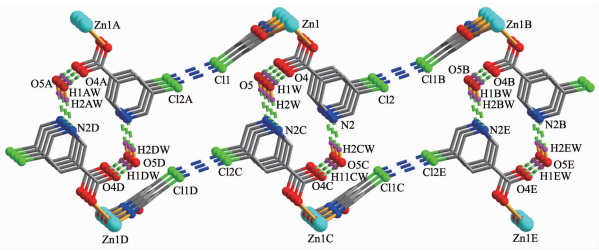

Phen ligands are omitted for clarity; Blue and green dashed lines represent Cl ⋯ Cl interactions and H-bonded, respectively; Symmetry codes: A: $x+1$, y, $z-1$; B: $x-1$, y, $z+1$; C: $-x+1$, $-y+1$, $-z+1$; D: $-x+2$, $-y+1$, $-z$; E: $-x+1$, $-y+1$, $-z+2$

Fig.9　Perspective of a 3D supramolecular framework along a axis

2.2 TGA analysis

To determine the thermal stability of compounds **1**~**4**, their thermal behaviors were investigated under nitrogen atmosphere by thermogravimetric analysis (TGA). As shown in Fig.10, polymer **1** lost its one and a half of lattice water molecules as well as a half of one H_2O ligand from 30 to 160 ℃ (Obsd. 8.7%; Calcd. 8.8%), followed by the decomposition at 329 ℃. For polymers **2** and **3**, the TGA curves revealed that their samples were stable up to 348 ℃ and 260 ℃, respectively, followed by a decomposition on further heating. The TGA curve of **4** showed that two lattice water molecules were released from 29 to 79 ℃ (Obsd. 5.8%; Calcd. 6.0%), and the dehydrated solid began to decompose at 278 ℃.

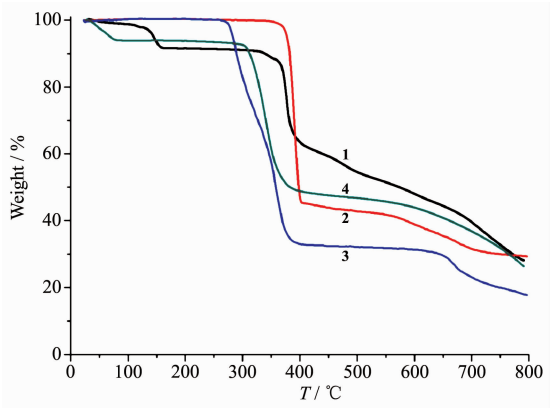

Fig.10 TGA curves of compounds **1**~**4**

2.3 Magnetic properties

Variable-temperature magnetic susceptibility studies were carried out on powder samples of **1** and **2** in a temperature range of 2~300 K. For the Ni(Ⅱ) MOF **1**, the $\chi_M T$ value at 300 K was 1.16 $cm^3 \cdot mol^{-1} \cdot K$, which was higher than the spin only value of 1.00 $cm^3 \cdot mol^{-1} \cdot K$ for one magnetically isolated Ni(Ⅱ) center ($S_{Ni}=1$, $g=2.0$). Upon cooling, the $\chi_M T$ value droped down very slowly from 1.16 $cm^3 \cdot mol^{-1} \cdot K$ at 300 K to 1.12 $cm^3 \cdot mol^{-1} \cdot K$ at 37 K and then decreased steeply to 0.26 $cm^3 \cdot mol^{-1} \cdot K$ at 2 K (Fig.11). The χ_M^{-1} vs T plot for **1** in the 3~300 K interval obeyed the Curie-Weiss law with a Weiss constant θ of −10.32 K and a Curie constant C of 1.19 $cm^3 \cdot mol^{-1} \cdot K$, suggesting a weak antiferromagnetic interaction between the Ni(Ⅱ) ions. Because of the long separation between the

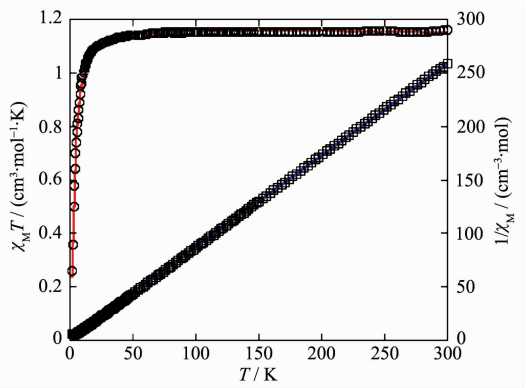

Red line represents the best fit to the equations in the text; Blue line shows the Curie-Weiss fitting

Fig.11 Temperature dependence of $\chi_M T$ (○) and $1/\chi_M$ (□) vs T for compound **1**

adjacent Ni_2 units, only the coupling interactions within the di-nickel(Ⅱ) blocks were considered.

We tried to fit the magnetic data of **1** using the following expression[25] for a dinuclear Ni(Ⅱ) unit:

$$H=-JS_1S_2$$

$$\chi_{M'}=\frac{N\beta^2 g^2}{3k(T-\theta)}\frac{\sum S'(S'+1)(2S'+1)e^{-E_s/(kT)}}{\sum(2S'+1)e^{-E_s/(kT)}}$$

$$\chi_M=\chi_{M'}(1-\rho)+\frac{4S(S+1)N\beta^2 g^2\rho}{3kT}+\mathrm{TIP}$$

where ρ is a paramagnetic impurity fraction and TIP is temperature independent paramagnetism. Using this model, the susceptibility for **1** above 2.0 K was simulated, leading to the values of $J=-2.53$ cm^{-1}, $g=2.11$, $\rho=0.005$, and TIP=9.04×10^{-6} $cm^3 \cdot mol^{-1}$, with the agreement factor $R=9.38\times10^{-4}$ ($R=\sum(T_{obs}-T_{calc})^2/\sum(T_{obs})^2$). The negative J parameter confirms that a weak antiferromagnetic exchange coupling exists between the adjacent Ni(Ⅱ) centers, which is in agreement with a negative θ value. In the structure of **1** (Fig.2), there are two types of magnetic exchange pathways within the dinuclear units, namely via the μ-H_2O and μ-η^1:η^1-carboxylate (*syn-syn*) bridges. According to previous studies, the magnetic interaction is highly sensitive to the value of the Ni-O-Ni bridging angle, showing the domination of the Ni-Ni ferromagnetic coupling when the Ni-O-Ni angles are (90±14)°[26]. The larger Ni-O-Ni angles in the Ni_2 unit (113.9(2)°) might suggest that the O bridges could be responsible for an antiferromagnetic exchange component. Meanwhile, the *syn-*

syn carboxylate group bridging is likely to have a dominant antiferromagnetic effect. Hence, the small $-J$ value observed for **1** (-2.53 cm^{-1}) could well be a result of two compatible exchange effects.

For **2**, the room temperature value of $\chi_M T$, 1.10 cm^3·mol^{-1}·K, was close to that of 1.00 cm^3·mol^{-1}·K expected for one magnetically isolated high-spin Ni(Ⅱ) ion (S=1, g=2.0). Upon cooling, the $\chi_M T$ value droped down very slowly from 1.10 cm^3·mol^{-1}·K at 300 K to 1.07 cm^3·mol^{-1}·K at 45 K and then decreased steeply to 0.53 cm^3·mol^{-1}·K at 2 K (Fig.12). Between **2** and 300 K, the magnetic susceptibilities can be fitted to the Curie-Weiss law with C=1.12 cm^3·mol^{-1}·K and θ=−9.14 K. These results indicate an antiferromagnetic interaction between the adjacent Ni(Ⅱ) centers in compound **2**. An empirical (Weng′s) formula can be applied to analyze the 1D systems with S=1, using numerical procedures[27-28]:

$$H=-JS_iS_j$$

$$\chi_M=\frac{N\beta^2g^2}{kT}\frac{A}{B}$$

$$A=2.0+0.019\ 4x+0.777x^2$$

$$B=3.0+4.346x+3.232x^2+5.834x^2$$

with $x=|J|/(kT)$

Using this method, the best-fit parameters for **2** were obtained: J=−1.91 cm^{-1}, g=2.05 and R=3.37×10^{-5}. A negative J parameter indicates a weak antiferromagnetic exchange coupling between the adjacent Ni(Ⅱ) centers in **2**, which is in agreement with a negative θ value.

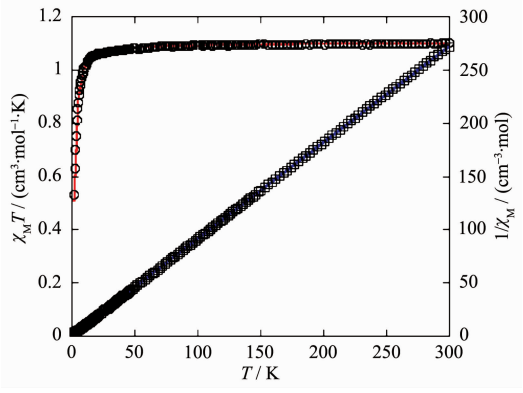

Red line represents the best fit to the equations in the text; Blue line shows the Curie-Weiss fitting

Fig.12 Temperature dependence of $\chi_M T$ (○) and $1/\chi_M$ (□) vs T for compound **2**

2.4 Luminescence properties

The emission spectra of 5-ClnicH and compounds **3** and **4** were measured in the solid state at room temperature, as depicted in Fig.13. The free 5-ClnicH ligand displayed a weak photoluminescence with an emission maximum at 452 nm. For compounds **3** and **4**, more intense emission bands are observed with maximum at 522 nm for **3** and 451 nm for **4** (λ_{ex}=305 nm in all cases). All bands can be assigned to an intraligand ($\pi^*\rightarrow n$ or $\pi^*\rightarrow\pi$) emission[11-13].

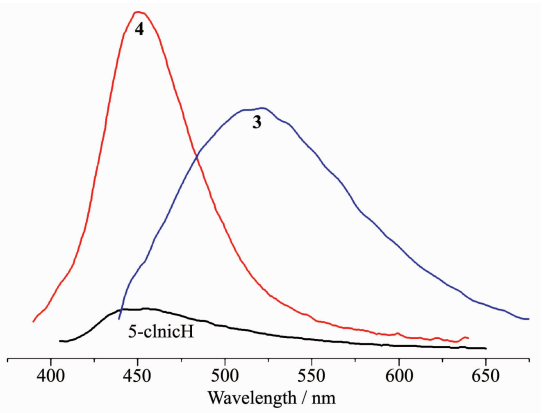

Fig.13 Solid state emission spectra of 5-ClnicH and compounds **3** and **4**

3 Conclusions

In this work, we applied an aqueous medium self-assembly method for the hydrothermal generation of four new coordination polymers derived from 5-chloronicotinic acid as a main building block. The obtained compounds were fully characterized and their structures range from 3D metal-organic framework (**1**) to 1D chain (**2**~**4**). The low dimensionality of **2**~**4** arises from the introduction of 2,2′-biimidazole and 1,10-phenanthroline as auxiliary ligands. Besides, the magnetic (for **1** and **2**) and Luminescent (for **3** and **4**) properties were also investigated and discussed. The results show that such simple, low-cost, and water-soluble carboxylic acid can be used as a versatile multifunctional building block toward the generation of new coordination polymers.

References:

[1] Lu W G, Su C Y, Jiang L, et al. *J. Am. Chem. Soc.*, **2006**,**128**:

34-35

[2] Zheng X D, Lu T B. *CrystEngComm*, **2010**,**12**:324-336

[3] Lee J Y, Farha O K, Roberts J, et al. *Chem. Soc. Rev.*, **2009**, **38**:1450-1459

[4] Cui Y J, Yue Y F, Chen B L. *Chem. Rev.*, **2012**,**112**:1126-1162

[5] Li J R, Kuppler R J, Zhou H C. *Chem. Soc. Rev.*, **2009**,**38**: 1477-1504

[6] Zhou Y L, Wu M C, Zeng M H, et al. *Inorg. Chem.*, **2009**, **48**:10146-10150

[7] Zhang L N, Zhang C, Zhang B, et al. *CrystEngComm*, **2015**, **17**:2837-2846

[8] Du M, Li C P, Liu C S, et al. *Coord. Chem. Rev.*, **2013**,**257**: 1282-1305

[9] Chen X M, Tong M L. *Acc. Chem. Res.*, **2007**,**40**:162-170

[10]Singh R, Bharatdwaj P K. *Cryst. Growth Des.*, **2013**,**13**:3722-3733

[11]Gu J Z, Gao Z Q, Tang Y. *Cryst. Growth Des.*, **2012**,**12**: 3312-3323

[12]Gu J Z, Cui Y H, Liang X X, et al. *Cryst. Growth Des.*, **2016**,**16**:4658-4670

[13]Gu J Z, Kirillov A M, Wu J, et al. *CrystEngComm*, **2013**,**15**: 10287-10303

[14]Wu Y P, Wu X Q, Wang J F, et al. *Cryst. Growth Des.*, **2016**,**16**:2309-2316

[15]Shao Y L, Cui Y H, Gu J Z, et al. *CrystEngComm*, **2016**,**18**: 765-7783

[16]Gao Z Q, Li H J, Gu J Z, et al. *J. Solid State Chem.*, **2016**, **241**:121-130

[17]Cui Y H, Wu J, Kirillov A M, et al. *RSC Adv.*, **2015**,**5**: 10400-10411

[18]Gu J Z, Cai Y, Liang X X, et al. *CrystEngComm*, **2018**,**20**: 906-916

[19]Spek A L. *Acta Crystallogr. Sect. C*: *Struct. Chem.*, **2015**,**71**: 9-18

[20]Van de Sluis P, Spek A L. *Acta Crystallogr. Sect. A*: *Found. Crystallogr.*, **1990**,**A46**:194-201

[21]LIANG Li-Li(梁丽丽), LIU Cong-Sen(刘从森), ZONG Zhi-Hui(宗智慧), et al. *Chinese J. Inorg. Chem.*(无机化学学报), **2018**,**34**(7):1365-1372

[22]Bertani R, Sgarbossa P, Venzo A, et al. *Coord. Chem. Rev.*, **2010**,**254**:677-695

[23]YAN Shi-Cheng(严世承), WU Da-Ling(武大令), ZHANG Min-Zhi(张敏芝), et al. *Chinese J. Inorg. Chem.*(无机化学学报), **2018**,**34**(6):1110-1120

[24]YANG Shi-Ying(杨诗吟), CAI Hua(才华), ZHANG Qi(张琦). *Chinese J. Inorg. Chem.*(无机化学学报), **2018**,**34**(1): 179-186

[25]Thompson L K, Niel V, Grove H, et al. *Polyhedron*, **2004**, **23**:1175-1184

[26]Mahata P, Natarajan S, Panissod P, et al. *J. Am. Chem. Soc.*, **2009**,**131**:10140-10150

[27]Kahn O. *Molecular Magnetism*. New York: VCH Publishers, **1993**.

[28]Weng C H. *Thesis for the Doctorate of Carnegie-Mellon University*. **1968**.